1-1-2020

A prospective study comparing tendon-to-bone interface healing using an interposition bioresorbable scaffold with a vented anchor for primary rotator cuff repair in sheep.

Jeremiah Easley
Colorado State University

Christian Puttlitz
Colorado State University

Eileen Hackett
Colorado State University

Cecily Broomfield
Colorado State University

Lucas Nakamura
Colorado State University

J Shoulder Elbow Surg (2020) 29, 157–166

ELSEVIER

Journal of Shoulder and Elbow Surgery

www.elsevier.com/locate/ymse

A prospective study comparing tendon-to-bone interface healing using an interposition bioresorbable scaffold with a vented anchor for primary rotator cuff repair in sheep

Jeremiah Easley, DVM[a], Christian Puttlitz, PhD[b], Eileen Hackett, DVM[a], Cecily Broomfield, MS[b], Lucas Nakamura, BS[b], Michael Hawes, DVM[c], Charles Getz, MD[d], Mark Frankle, MD[e,f], Patrick St. Pierre, MD[g], Robert Tashjian, MD[h], P. Dean Cummings, MD[i], Joseph Abboud, MD[j], Derek Harper, BSE[k], Kirk McGilvray, PhD[b,*]

[a]*Preclinical Surgical Research Laboratory, Colorado State University, Fort Collins, CO, USA*
[b]*Orthopedic Bioengineering Research Laboratory, Colorado State University, Fort Collins, CO, USA*
[c]*Charter Preclinical Services, Hudson, MA, USA*
[d]*Orthopedic Surgery, Thomas Jefferson University, Philadelphia, PA, USA*
[e]*Florida Orthopaedic Institute, Shoulder and Elbow Service, Tampa, FL, USA*
[f]*Morsani College of Medicine, University of South Florida, Tampa, FL, USA*
[g]*Shoulder and Elbow Service, Desert Orthopedic Center, Eisenhower Health, Rancho Mirage, CA, USA*
[h]*University of Utah School of Medicine, Salt Lake City, UT, USA*
[i]*The Orthopedic Clinic Association, Phoenix, AZ, USA*
[j]*The Sidney Kimmel Medical College, Thomas Jefferson University, Philadelphia, PA, USA*
[k]*Zimmer Biomet, Warsaw, IN, USA*

Background: The purpose of this study was to evaluate the biomechanical and histologic properties of rotator cuff repairs using a vented anchor attached to a bioresorbable interpositional scaffold composed of aligned PLGA (poly(L-lactide-*co*-glycoside)) microfibers in an animal model compared to standard anchors in an ovine model.

Methods: Fifty-six (n = 56) skeletally mature sheep were randomly assigned to a repair of an acute infraspinatus tendon detachment using a innovative anchor-PLGA scaffold device (Treatment) or a similar anchor without the scaffold (Control). Animals were humanely euthanized at 7 and 12 weeks post repair. Histologic and biomechanical properties of the repairs were evaluated and compared.

Results: The Treatment group had a significantly higher fibroblast count at 7 weeks compared to the Control group. The tendon bone repair distance, percentage perpendicular fibers, new bone formation at the tendon-bone interface, and collagen type III deposition was significantly greater for the Treatment

This study was conducted under Institutional Animal Care and Use Committee approval (Colorado State University 15-5611A).

*Reprint requests: Kirk McGilvray, PhD, 1374 Campus Delivery, Fort Collins, CO 80523, USA.
E-mail address: kirk.mcgilvray@colostate.edu (K. McGilvray).

https://doi.org/10.1016/j.jse.2019.05.024

group compared with the Control group at 12 weeks ($P \leq .05$). A positive correlation was identified in the Treatment group between increased failure loads at 12 weeks and the following parameters: tendon-bone integration, new bone formation, and collagen type III. No statistically significant differences in biomechanical properties were identified between Treatment and Control Groups ($P > .05$).

Conclusions: Use of a vented anchor attached to a bioresorbable interpositional scaffold composed of aligned PLGA microfibers improves the histologic properties of rotator cuff repairs in a sheep model. Improved histology was correlated with improved final construct strength at the 12-week time point.

Level of evidence: Basic Science Study; Biomechanics and Histology

Keywords: Rotator cuff repair; rotator cuff tendon; PLGA scaffold; suture anchor; biomechanics; histology; ovine

Rotator cuff tendon tears are common and represent the most common shoulder injury for patients requiring surgical treatment. An estimated 450,000 rotator cuff repairs are performed in the United States per year.[42] With an aging population (>60 years of age) and increasing frequency of tearing, the need for repair is expected to continue to grow.[6,16,19,45] Patients affected by a rotator cuff tear often demonstrate limited shoulder mobility, reduced strength, and pain. Successful rotator cuff repair can be challenging, especially in chronic situations where poor tendon and bone are present. Numerous factors are associated with impaired healing, such as poor tendon quality and vascularity, muscle atrophy, and fatty infiltration.[3,7,11-13,26,47] Additional patient factors such as systemic medical morbidities, including diabetes and tobacco use, can result in high rates of repair failures, with structural failure ranging from 30% to as high as 94%.[1,11,13] The goal of a rotator cuff repair is to form an enthesis (or a stable mechanical attachment of the muscle-tendon unit to the bony attachment site on the proximal humerus) that mimics the mechanical function of the native tendon-to-bone interface. Traditional techniques have mainly focused on improving the mechanical attachment of the tendon-bone interface, with less emphasis on improved biological healing; however, biological healing is critical to achieve a durable union at the tendon-bone interface.

Various techniques have been employed to improve interface healing, including bone marrow venting; cellular therapies (mesenchymal stem cells); and xenograft, allograft, or acellular scaffolds.[27,29,32,36,41] Bone marrow vents have shown promise in improving the bone-tissue interface healing of many soft tissue injuries by allowing autologous marrow-derived cells to reach the repair site.[9,37] Bone marrow venting is a comparatively expeditious surgical procedure, has no issue of cellular incompatibility, and may be accomplished through vented tissue anchors or through separate bone puncture holes.[9,46] Potential problems with bone puncture holes for bone marrow venting is that it can weaken the bone around the venting holes, possibly leading to inadequate anchor fixation in the bone.[37]

Scaffolds or "patches" have also shown value for augmenting torn tissue and promoting tissue thickening.[32,41] Tissue thickening has been demonstrated to have a beneficial effect on the inherent mechanical strength of the repair.[38,41] Most scaffolds are placed on top of the tendon (ie, onlay), not as an interposition between the tendon and the bone, and are primarily designed to add initial mechanical strength and surface area to the repair site, potentially reducing and preventing tendon retear and retraction from the footprint.[14,32] Recently, interest in interposition (ie, inlay—between the tendon and bone at the footprint) patches has increased as it is believed to not only improve the strength of the repair site, similar to onlay scaffolds but also lead to increased bone-tendon integration via increased cellular activity. The mechanism of action of interposition patches is thought to be conveyed by increasing the biomechanical properties of the repair via the cellular response to the scaffold.[36]

Because of the potential benefits observed with these surgical techniques (ie, bone venting and interposition scaffold augmentation), it was hypothesized that a combination of a marrow venting anchor, with an attached interposition scaffold, may be advantageous to rotator cuff repair healing. Therefore, the purpose of this study was to compare the healing rates, biomechanical strength, and histologic properties of rotator cuff repairs performed using a vented anchor attached to a bioresorbable interpositional scaffold composed of aligned PLGA (poly(L-lactide-*co*-glycolide)) microfibers to repairs performed using standard suture anchors. A previously investigated sheep rotator cuff model from our research group was used as the animal model.[14,17,18,31-35,40,41]

Materials and methods

Vented suture anchor with PLGA scaffold

The suture anchor with incorporated PLGA scaffold is composed of 2 components: the anchor construct and the scaffold construct,

which is integrated into the anchor construct (BioWick SureLock W Suture Anchor, Zimmer-Biomet, Warsaw, IN). The suture anchor implant is an all-suture anchor construct with braided ultrahigh-molecular-weight polyethylene suture fibers, and a polyether ether ketone anchor component that serves to house and protect the scaffold and suture components. The scaffold component is a porous, aligned fiber matrix composed of 1-μm-diameter PLGA fibers produced using electrospinning techniques. The dimensions of the scaffold were 8 mm × 8 mm × 420 μm (height × width × thickness). We hypothesized that the porous nature of the scaffold allows for the essential for cell nutrition, proliferation, and migration during the healing process, permitting infiltration and ingrowth of fibroblasts. Additionally, the pores and aligned fibers should assist in guiding new fibroblast orientation, enabling effective release of biofactors such as proteins, genes, or cells.[20] The PLGA scaffold is manufactured using standard electrospinning fabrication techniques, a process used to make small-diameter fibers using a high electric potential to draw charged polymer solutions to fiber sizes ranging from nanometers to micrometers, depending on the desired application.

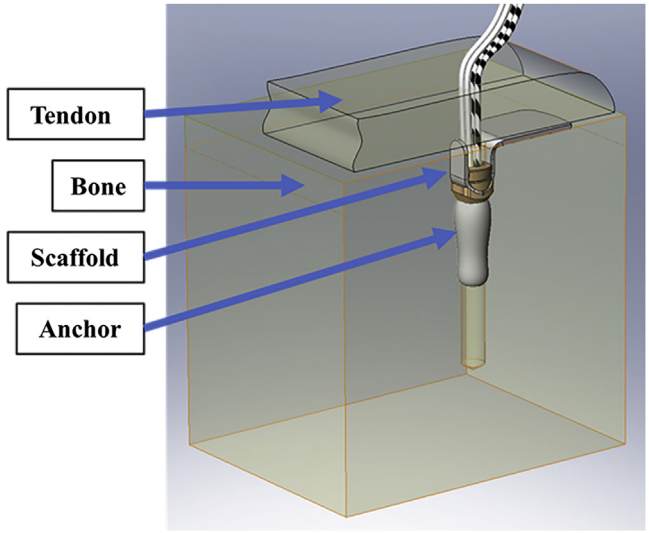

Figure 1 Architecture of the new anchor-scaffold device.

Sample size calculation

A power analysis was performed using pilot biomechanical stiffness data (unpublished) examining acute rotator cuff tendon repairs in an ovine model. Two-sample *t*-test power calculation indicated that n = 7.04 (where δ = 6.48, SD = 3.06, bilevel = 0.01, power = 0.8; alternative = 2-sided) were needed per group to achieve statistical fidelity of post hoc analysis.

Animal procedures

Fifty-six (n = 56) skeletally mature female Columbia Cross sheep (*ovis aries*) (65-115 kg) were randomly assigned to treatment groups (ie, new anchor-PLGA scaffold device "Treatment" or predicate device "Control") and survival times of either 7 or 12 weeks. The sheep infraspinatus tendon acute transection/repair model was used as previous studies have demonstrated that it is a good analog for the human supraspinatus tendon.[14,17,18,31-35,40,41] Using an open approach, the infraspinatus tendon was sharply detached from the humeral footprint followed by removal of any remaining soft tissue from the footprint by a bone burr. Repair or reattachment of the transected tendon was immediately performed using a total of two 2.7-mm suture anchors (BioWick SureLock W Suture Anchor; Zimmer-Biomet, Warsaw, IN, USA) with a PLGA scaffold (ie, Treatment group) (Fig. 1) or without a PLGA scaffold (Control group) (SureLock All-Suture Anchor; Zimmer-Biomet) and two 2.2-mm suture anchors (SureLock All-Suture Anchor) in a repair construct as described by Lorbach et al[22] using a modified double-row technique. During implantation, the anchor with the integrated PLGA scaffold was oriented laterally such that the scaffold lay on the humeral footprint (ie, inlay position) aligned with the desired direction of the healing tendon fibers prior to reattachment of the infraspinatus tendon. Following reattachment of the infraspinatus tendon, the acromial head of the deltoid muscle was returned to its more cranial position and the deltoid fascia and subcutaneous tissues were closed using a simple continuous suture pattern, and the skin was routinely closed with stainless steel staples. Following recovery, the sheep could move and eat *ad libitum* for the entirety of the study period. At 7 or 12 weeks, a total of 28 sheep were humanely euthanized with an overdose of barbiturate. Once euthanized, the infraspinatus muscle was isolated and detached from the scapula and the proximal one-third of the humerus was harvested. A total of 13 contralateral untreated shoulders were also randomly collected from sheep to serve as time zero baseline biomechanical and histologic samples.

Harvested humerus-infraspinatus constructs underwent fine dissection to remove any extraneous soft tissues, isolating the tendon from the infraspinatus muscle belly. Repair sutures were left intact following fine dissection. Sixteen (n = 16) samples were allocated for biomechanical testing (n = 8 Treatment and n = 8 Control samples) and 12 (n = 12) samples were allocated for histologic analysis (n = 6 Treatment, and n = 6 Control samples) for each timepoint. Those performing post-euthanization analyses were blinded to treatment groups and euthanizing timepoints until final statistical analyses were performed.

Destructive biomechanical testing

Samples allocated to biomechanical testing underwent cross-sectional area (CSA; mm^2) measurements of each infraspinatus tendon using an area micrometer (0.0245-mm^2 resolution). To ensure repeatability across samples, area measurements were taken while a 0.12-MPa pressure was applied parallel to the cross section of the tendon without application of axial load to the tendon.[25] Measurements of cross-sectional area were performed at multiple locations (n = 3) along the tendon (distal, middle, and proximal to the humeral attachment of the tendon), and the geometric mean was calculated as the representative CSA. CSA measurements were used to transform structural properties into material properties by normalizing for cross-sectional area thickening in the healing tendon (ie, calculating elastic modulus [MPa] from stiffness [N/mm] and stress [MPa] from load [N]).

After measurement of CSA, the humerus of each sample was potted within a poly-vinyl-composite (PVC) sleeve, using a 2-part epoxy resin (Smooth Cast 321; Smooth-on Inc., Easton, PA, USA). Specimens were mounted on a servo-hydraulic testing

machine (MiniBionix 858; MTS Systems, Eden Prairie, MN, USA) using specially designed fixtures (Fig. 2).[32] An upper fixture grip attached to the MTS machine's actuator was used to clamp onto the infraspinatus tendon with a brass grip. Solid carbon dioxide was laid around the brass clamp to convert it into a cryo-clamp, lowering the temperature to at least –10°C for biomechanical testing.[32]

Destructive biomechanical testing included 2 phases: (first) preconditioning and (second) ramp to failure. Ramp to failure was a destructive test and was performed as the last test in the evaluation sequence. To minimize the viscoelastic effects on the measured biomechanical response, 10 cyclic tensile loads ranging between 0 and 2% strain were applied for the purpose of preconditioning the tendon. The preconditioning phase was preceded by a 2-minute preload phase. A static preload of 10 N was applied to all specimens for 2 minutes or until the specimen was fully relaxed. The sample's reference gauge length was measured as the tendon's distance (mm) from the bottom of the cryo-clamp's grip to the tendon's insertion into the humerus following the 10-N preload. All ramp to failure loads imparted on the samples were applied quasi-statically (100 mm/min) and aligned collinear to the physiologic loading direction of the tendon. Structural properties representing the biomechanical behavior of the bone-tendon construct and material properties representing the biomechanical behavior at the tissue level were calculated. Force (N) and displacement (mm) data were collected at 100 Hz and used to characterize structural properties of the tendon-bone construct and included ultimate load and stiffness. Material properties were calculated from structural measurements by normalization to cross-sectional area (mm^2) or to the initial gauge length (mm) of the sample and included ultimate stress and elastic modulus.

Histologic analysis

Samples (humeral-infraspinatus constructs) allocated to histologic process were fixed in 10% neutral-buffered formalin (≥7 days). Samples were bisected through the infraspinatus and humeral attachment sites creating a 1-cm-thick slab of tissue encompassing the bone-tendon repair site (ie, the ''footprint''). Samples underwent a standard decalcification process with 8% formic acid, followed by paraffin embedding. Two (n = 2) regions of interest, separated by 2000 μm, were examined across the footprint to determine the average histopathologic response at the repair site. Eight serial slide sections (5-μm-thick) were cut on a rotary microtome from the region of interest, with 2 (n = 2) slides from each region of interest being stained with (1) hematoxylin and eosin (H&E), (2) picrosirius red, (3) safranin O/fast green, or (4) unstained for immunohistochemistry collagen I and III analyses. Slides were evaluated by a board-certified veterinary pathologist using a modified ISO-1099/6 scoring rubric for 10 metrics, specifically:

1. Inflammation (0-5 score; 0 = no inflammation and 5 = severe inflammation)
2. Fibroblast count (n)
3. Tendon-bone repair distance (mm). For this measurement, the entire distance of the potential humeral insertion surface for the repaired infraspinatus tendon was measured. Landmarks used included the infraspinatus bursa on one end and the end of the humerus bone on the slide on the other end. Picrosirius red–stained slides were used to generate these data.
4. Movin' tendinopathy (0-3 score; 0 = normal and 3 = markedly abnormal). Movin' tendinopathy was a cumulative scoring of the tendon's fiber structure, fiber arrangement, rounding of nuclei, regional variation in cellularity, increased vascularity, and decreased collagen stainability, with each constituent being scored on a 3-point scale and then averaged across a single sample.[29]
5. Area of new fibrocartilage (mm^2)
6. Percentage tendon-bone integration (%)
7. Percentage perpendicular oriented fibers (%)
8. Collagen I content (0-10 score; 0 = no indication and 10 = strong (+4) signal)
9. Collagen III content (0-10 score; 0 = no indication and 10 = strong (+4) signal)
10. New bone formation at tendon-bone interface (mm^2)

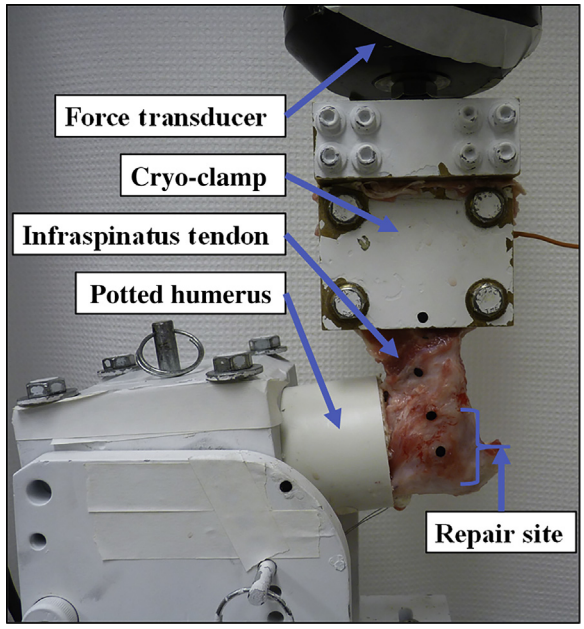

Figure 2 Digital image of the testing fixture. A representative infraspinatus tendon prior to destructive biomechanical testing is shown.

Fibroblasts were counted in 4× to 40× objective fields from H&E sections within 8 mm of the PLGA scaffold when present or within 10 mm of bone-tendon interface when the PLGA scaffold was absent.

Statistical analysis

Statistical significance in the biomechanical and histopathologic output parameters between groups and across time points was performed using a standard 2-way analysis of variance for multiple comparisons, where P values less than .05 were considered statistically significant (Minitab, Inc, State College, PA, USA). Untreated data were not included in the statistical analyses; however, the data are presented as a measure of baseline values. An analysis comparing the histopathology and

biomechanical results was performed using Pearson correlation analyses. Within a Pearson product-moment correlation, the pair(s) of variables with positive correlation coefficients and P values $<.05$ tend to increase together. For the pairs with negative correlation coefficients and P values $<.05$, one variable tends to decrease whereas the other increases. For pairs with P values $>.05$, there is no significant relationship between the 2 variables.

Results

All sheep tolerated the surgery well and without complication. A single sheep had mild signs of lameness in the treated limb at 10 days postoperation that resolved within 3 days of nonsteroidal anti-inflammatory drug therapy. No other clinical signs of postoperative pain, infection, or incision dehiscence were noted throughout the entirety of the study period.

Data figures are shown in box and whisker plot format. The ''box'' is bounded by the first and third quartiles; the ''whiskers'' represent the maximum/minimum values within the data set, and the median data bar is highlighted. Statistically significant differences have been highlighted; means that do not share a letter are significantly different.

Histologic results

Histopathology did not indicate any abnormal or adverse reaction or immune response in either surgical group. Qualitatively, tendon repair progressed in an expected fashion from 7 to 12 weeks in both groups. Inflammation scores for the Treatment group at both 7 and 12 weeks were modestly reduced compared to the Control group's (Fig. 3, *I*). Minimal to mild chronic inflammation and perivascular inflammation was present in both Treatment and Control groups at both 7 and 12 weeks.

As expected, all Treatment and Control fibroblast counts were significantly increased compared to untreated controls, and sum fibroblast counts subsided over time in both groups (Fig. 3, *II*).

Tendon-bone repair distance was a measurement of the entire distance of the potential humeral insertion surface for the repaired infraspinatus tendon from picrosirius red sections. The tendon-bone repair distance was significantly greater for the 12-week Treatment group compared with the Control group at 12 weeks, and the Treatment and Control groups at 7-weeks (Fig. 3, *III*).

Movin' tendinopathy scores were generated from evaluation of H&E and picrosirius red sections on a scale from 0-3 for fiber structure, fiber arrangement, rounding of nuclei, regional variations of cellularity, increased vascularity, and decreased collagen stainability. No significant differences were noted between the Treatment and Control groups within either euthanizing time point based on Movin' total sum scores. Movin' scores significantly subsided over time in both groups from 7 to 12 weeks (Fig. 3, *IV*).

Areas of safranin O–positive metachromatic tissue (Fig. 4) that were consistent with fibrocartilage were measured at the infraspinatus tendon-bone interface in mm^2. No significant differences in area of new fibrocartilage at the tendon-bone interface was noted between or within groups at either time points (Fig. 3, *V*).

Percentage tendon-bone integration with any tissue was calculated by dividing the total tendon-bone integration distance (mm) by the total tendon-bone repair distance (mm). Percentage tendon-bone integration was significantly increased in the Treatment group compared to the Control group at 12 weeks (Fig. 3, *VI*).

The percentage of tendon-bone integration distance (with respect to any tissue type) occupied by perpendicular fibers was calculated by dividing the distance (mm) fibers were attached to the bone perpendicularly ($\pm 10^{\circ}$) by the tendon-bone integration distance (mm). Percentage tendon-bone integration with perpendicular fibers were significantly increased in the Treatment group compared to the Control group at 12 weeks (Fig. 3, *VII*).

Collagen I and III content was scored on a scale from 0-10. Collagen I scores were comparable and stable across the 7- and 12-week time points in the Treatment and Control groups (Fig. 3, *VIII*). Collagen III scores ''near'' the PLGA in the Treatment group at 7 and 12 weeks were modestly increased compared with their respective 7- and 12-week controls at the tendon-bone interface (Fig. 3, *IX*). In addition, there was a statistically significant increase in collagen type III deposition in the Treatment group as compared to the Control group at 12 weeks (Fig. 3, *IX*).

Additionally, the Treatment group had a significant increase in new bone formation at the tendon-bone interface compared with the Control group at 12 weeks (Fig. 3, *X*).

For completeness, the untreated samples demonstrated significant reductions in all histopathologic parameters compared with either the Treatment or Control groups at either the 7- or 12-week time points (Fig. 3; $P \leq .05$ for all comparisons [not shown]).

Biomechanical results

No grossly abnormal pathologies or abnormal tissue reactions were noted at the time of dissection. No experimental issues were noted; all biomechanical tests were run to completion.

There were no significant differences noted in CSAs of the infraspinatus tendons across groups at 7 or 12 weeks ($P > .05$). No significant differences were noted between the Treatment and Control groups within the 7-week or 12-week time points with regards to ultimate failure load (N) ($P \geq .55$), construct stiffness (N-m) ($P \geq .70$), ultimate failure stress (MPa) ($P \geq .93$), or elastic modulus (MPa) ($P \geq .56$) (Fig. 5). However, significant differences across time points (ie, 7 weeks vs. 12 weeks) were observed for all biomechanical output parameters (Fig. 5). For all

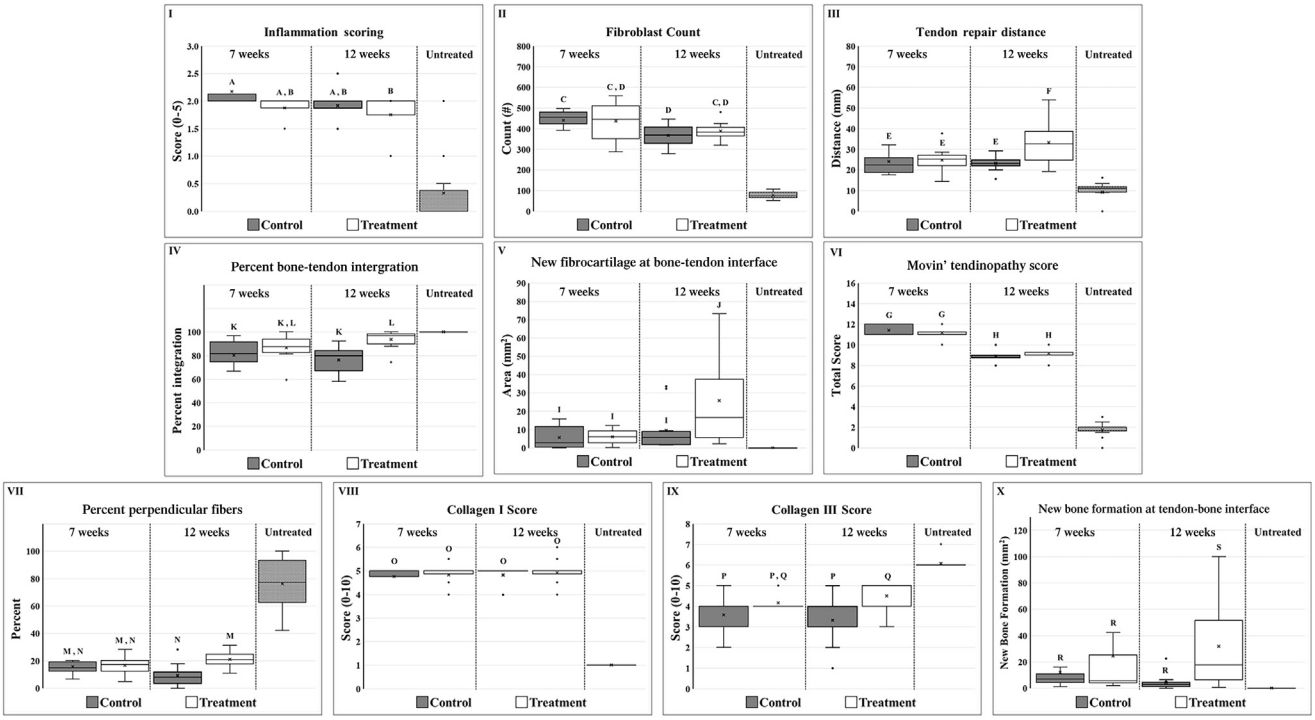

Figure 3 Histopathologic scoring of tendon repair. Statistically significant differences have been highlighted; means that do not share a letter are significantly different. (**I**) A-B: P value $\leq$ .046; (**II**) C-D: P value $\leq$ .041; (**III**) E-F: P value $\leq$ .011; (**IV**) G-H: P value $\leq$ .001; (**V**) I-J: P value $\leq$ .043; (**VI**) K-L: P value $\leq$ .029; (**VII**) M-N: P value $\leq$ .050; (**VIII**) O: P value $\geq$ .714; (**IX**) P-Q: P value $\leq$ .046; (**X**) R-S: P value $\leq$ .050.

biomechanical output parameters, the data indicated statistically significant increases for both surgical groups at the 12-week time point as compared to both groups at the 7-week time point (Fig. 5). The biomechanical responses of the untreated samples demonstrated increased responses in all measured parameters as compared to both surgical groups at both time points (Fig. 5).

The Pearson correlation analyses between the histopathology and biomechanical results showed a statistically significant, positive, correlation in the Treatment group between increased failure loads at 12 weeks and the following parameters: tendon-bone integration ($R^2 = 0.83$, P value = .02), and collagen type III ($R^2 = 0.85$, P value = .01).

Discussion

This study successfully evaluated a new commercially available, FDA-approved PLGA scaffold device that is incorporated into a vented suture anchor implant for rotator cuff repair in sheep. To our knowledge, this is the first vented suture anchor with an engineered interpositional scaffold for rotator cuff repair. The devices were easy to implant and required no additional steps from the traditional repair technique. Additionally, the devices used in this study could have been implanted using either open surgical or arthroscopic techniques. The data indicated that there were no persistent test article–related toxicologically relevant histopathologic findings relative to the control devices.

The results suggest that the PLGA scaffold has a positive biomimetic effect on the healing quality of infraspinatus tendon to bone following an acute transection and reattachment in a sheep model. Statistical improvements in tendon-bone distance, percentage tendon-bone integration, and percentage tendon-bone integration distance suggest that the PLGA scaffold has a measurable, positive effect on the histopathologic quality of tendon repair. Because both anchors were vented, it is likely that the PLGA scaffold is responsible for improved healing parameters. In addition, because both anchors were vented, this study design was unable to explicitly assess the effect the anchor's vent had on the healing rate. The microfibers of the aligned PLGA scaffold are intended to mimic the extracellular matrix (collagen) of the native rotator cuff tendon. It has been shown that randomly oriented fibers result in more random fibroblast orientation.[10] Therefore, we believe that the fiber alignment of the PLGA scaffold is likely to play a role in the outcomes noted in this study. Furthermore, nonsignificant differences in inflammation and Movin' tendinopathy scores suggest that the addition of the PLGA scaffold has no negative affect on tendon healing.

The ultimate failure loads reported within this study were significantly greater than previously published results

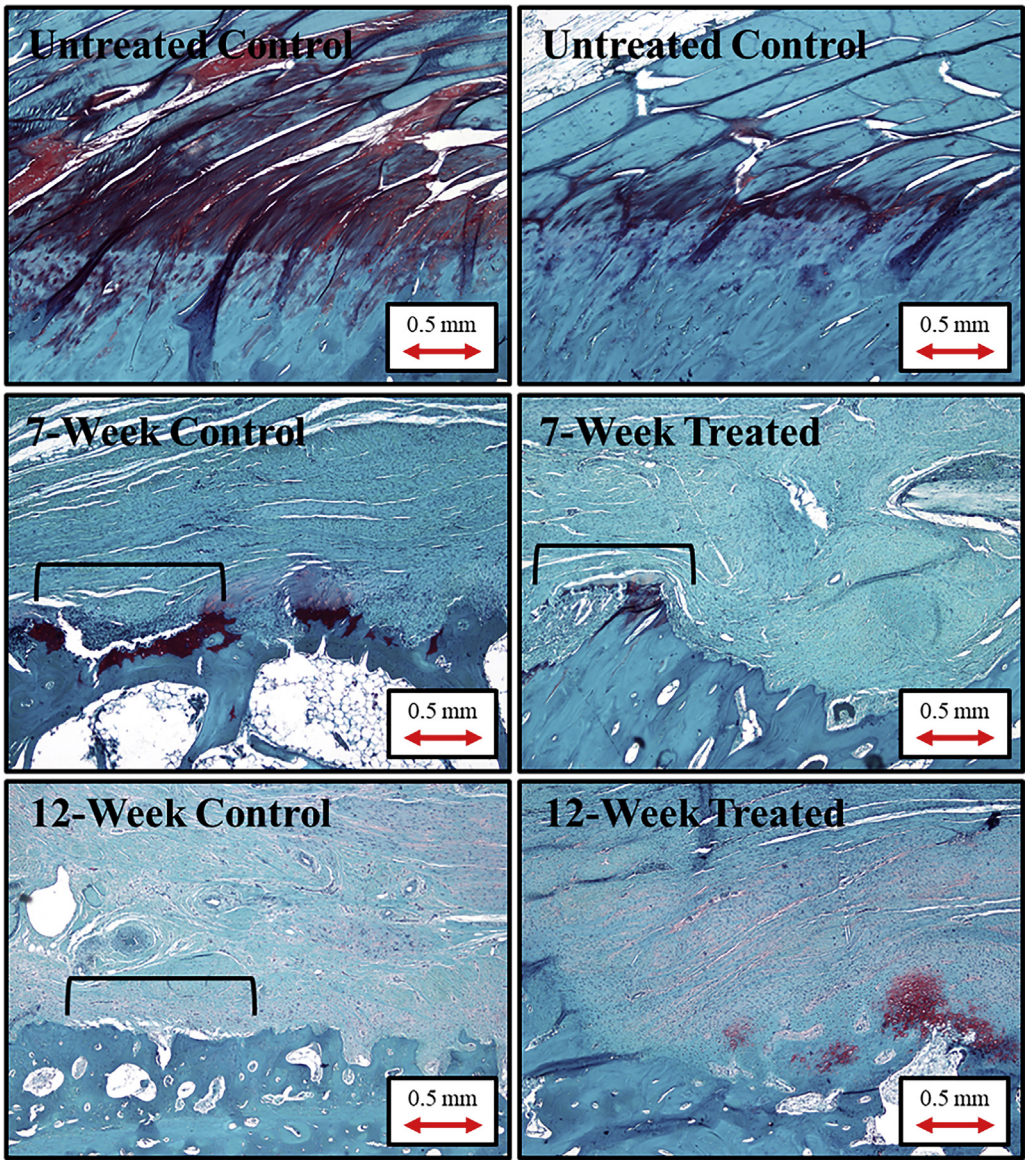

Figure 4 Untreated, control, and treated infraspinatus tendon repair sites at 7 and 12 weeks: these images show the tissue integration at the tendon-bone interface. Black brackets denote areas where the repair tissue is not well integrated with the bone. Safranin O stain; 40× magnification.

using the same acute transection ovine model. Work by Hee et al[14] reported ultimate failure loads of 910.4 ± 156.1 N for suture-only controls, compared with the ultimate failure loads of 1758 ± 750 N found in this study using equivalent biomechanical testing protocols. The main difference between this study and the work by Hee et al is the difference in suture patterns (ie, bridging technique with bone anchors vs. a modified Mason-Allen with bone tunnels, respectively) and the vented anchor design. These data, perhaps in absolute terms, may help corroborate the data presented by others demonstrating the significant effect that acute suture purchase (ie, technique) has on the ultimate strength of the repair[4,21,39,43] and the importance of allowing cellular constituents to reach the repair site.

The sheep acute rotator cuff model is well established and is considered an acceptable model for device testing because of anatomical similarities to humans.[15,28,44] Because of the similarities (ie, anatomical features, in vivo biomechanical loading, bone composition and structure, etc) between humans and sheep, we believe that it is acceptable to conjecture that increased biomechanical and histopathologic results between treatment groups detected within this study in the in vivo ovine model would correspond to the increases in repair results observed between treatment groups in human subjects. However, the ovine model is not without limitations.[29,32,40] Most notably, the inability to limit weight bearing in a quadrupedal animal can lead to gap formation at the tendon-bone interface. Recently, human studies have shown similar gap formations to occur when repairs to the RTC are loaded acutely.[24] Also, because both implants had a vented design, the data were incapable of clarifying if the anchor's venting was explicitly advantageous. However, the

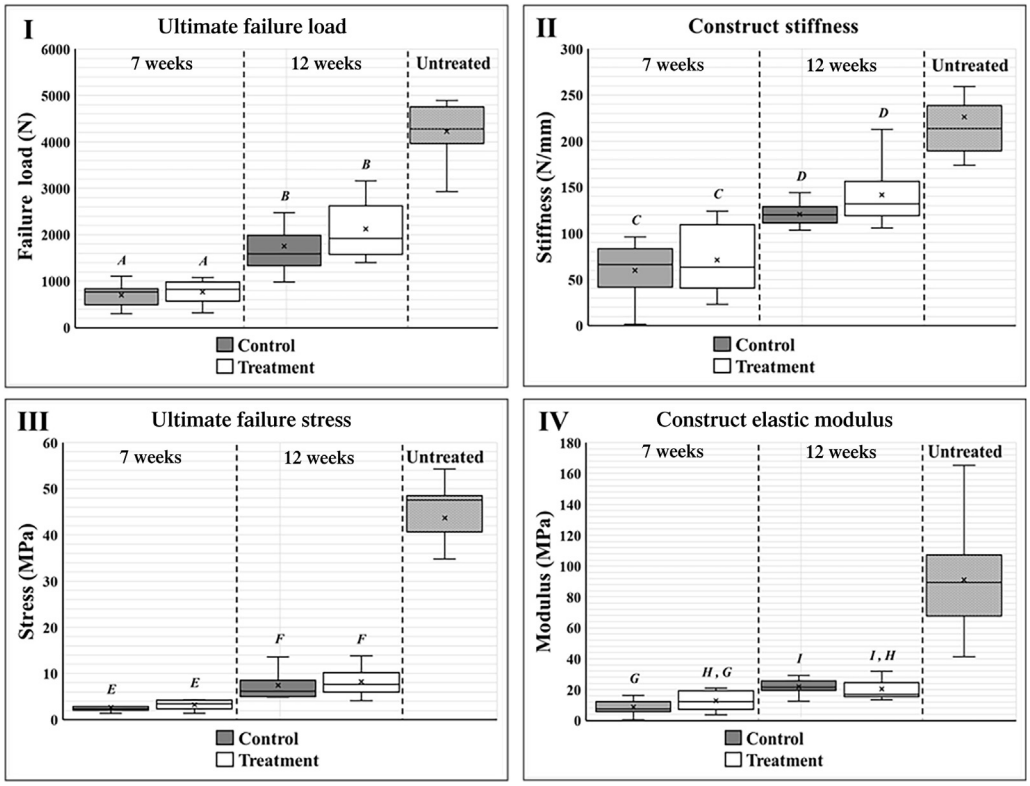

Figure 5 Biomechanical response following quasi-static ramp to failure testing of the surgically repaired infraspinatus tendon. Statistically significant differences have been highlighted; means that do not share a letter are significantly different. (**I**) A-B: P value $\leq$ .006; (**II**) C-D: P value $\leq$ .020; (**III**) E-F: P value $\leq$ .008; (**IV**) G-H: P value $\leq$ .004; G-I: P value $\leq$ .001; H-I: P value $\leq$ .032.

data did indicate that the PGLA scaffold in conjunction with a vented anchor had significant positive effects on the healing. Lastly, this study used an acute repair model, whereas rotator cuff tears in people are often chronic and repair occurs after chronic changes have occurred to tendon, muscle, and bone. However, research has shown that sheep rotator cuff muscle undergoes similar chronic degradation, including muscle fatty infiltration and fibrosis, in situations of acute repair.[5,23] Regardless, we realize a limitation of this study is that the results have not been assessed for human clinical benefit in a large human patient population. Future studies in large patient populations would ultimately be needed to determine the device's effectiveness in terms of outcomes and quality of life postoperation.

There is a clear need for improving rotator cuff repair strategies based on the high repair failure rates in patients.[1,11,13] Scaffold devices, derived from mammalian extracellular matrix (EM) and/or synthetic polymers, are becoming increasingly popular to potentially enhance the intrinsic healing potential of the tendon.[2,8,30] Many serve to mechanically ''off-load'' the repair in the early healing phases by increasing the tendon-bone contact, while others serve to biologically improve the rate and quality of healing. The overarching goal of all devices is to improve the quality and speed of healing. A scaffold, like the one used in this study, that would serve to enhance biological healing without requiring additional surgical steps or the implantation of additional devices would be appealing and have a potentially positive impact in rotator cuff repair outcomes.

Conclusion

Use of a vented anchor attached to a bioresorbable interpositional scaffold composed of aligned PLGA microfibers improves the histologic properties of rotator cuff repair in a sheep model. Improved histology is correlated with improved final construct strength. Use of a vented anchor in combination with an interpositional PLGA scaffold may improve tendon healing and strength for rotator cuff repair. Future clinical studies are needed to confirm these improved healing properties in the human population.

Acknowledgments

This work was funded by a grant from Zimmer Biomet, Warsaw, IN, USA, to Colorado State University, Fort Collins, CO, USA.

Disclaimer

The authors, their immediate families, and any research foundations with which they are affiliated have not received any financial payments or other benefits from any commercial entity related to the subject of this article.

References

1. Ahmad S, Haber M, Bokor DJ. The influence of intraoperative factors and postoperative rehabilitation compliance on the integrity of the rotator cuff after arthroscopic repair. J Shoulder Elbow Surg 2015;24:229-35. https://doi.org/10.1016/j.jse.2014.06.050
2. Aurora A, McCarron J, Iannotti JP, Derwin K. Commercially available extracellular matrix materials for rotator cuff repairs: state of the art and future trends. J Shoulder Elbow Surg 2007;16:S171-8. https://doi.org/10.1016/j.jse.2007.03.008
3. Boileau P, Brassart N, Watkinson DJ, Carles M, Hatzidakis AM, Krishnan SG. Arthroscopic repair of full-thickness tears of the supraspinatus: does the tendon really heal? J Bone Joint Surg Am 2005;87:1229-40. https://doi.org/10.2106/jbjs.D.02035
4. Cole BJ, ElAttrache NS, Anbari A. Arthroscopic rotator cuff repairs: an anatomic and biomechanical rationale for different suture-anchor repair configurations. Arthroscopy 2007;23:662-9. https://doi.org/10.1016/j.arthro.2007.02.018
5. Coleman SH, Fealy S, Ehteshami JR, MacGillivray JD, Altchek DW, Warren RF, et al. Chronic rotator cuff injury and repair model in sheep. J Bone Joint Surg Am 2003;85:2391-402. https://doi.org/10.1016/0020-1383(86)90112-9
6. Colvin AC, Egorova N, Harrison AK, Moskowitz A, Flatow EL. National trends in rotator cuff repair. J Bone Joint Surg Am 2012;94:227-33. https://doi.org/10.2106/JBJS.J.00739
7. Deprés-Tremblay G, Chevrier A, Snow M, Hurtig MB, Rodeo S, Buschmann MD. Rotator cuff repair: a review of surgical techniques, animal models, and new technologies under development. J Shoulder Elbow Surg 2016;25:2078-85. https://doi.org/10.1016/j.jse.2016.06.009
8. Derwin KA, Codsi MJ, Milks RA, Baker AR, McCarron JA, Iannotti JP. Rotator cuff repair augmentation in a canine model with use of a woven poly-L-lactide device. J Bone Joint Surg Am 2009;91:1159-71. https://doi.org/10.2106/JBJS.H.00775
9. Dierckman BD, Ni JJ, Karzel RP, Getelman MH. Excellent healing rates and patient satisfaction after arthroscopic repair of medium to large rotator cuff tears with a single-row technique augmented with bone marrow vents. Knee Surg Sports Traumatol Arthrosc 2018;26:136-45. https://doi.org/10.1007/s00167-017-4595-6
10. Erisken C, Zhang X, Moffat KL, Levine WN, Lu HH. Scaffold fiber diameter regulates human tendon fibroblast growth and differentiation. Tissue Eng Part A 2013;19:519-28. https://doi.org/10.1089/ten.tea.2012.0072
11. Galatz LM, Ball CM, Teefey SA, Middleton WD, Yamaguchi K. The outcome and repair integrity of completely arthroscopically repaired large and massive rotator cuff tears. J Bone Joint Surg Am 2004;86:219-24.
12. Gerber C, Meyer DC, Schneeberger AG, Hoppeler H, von Rechenberg B. Effect of tendon release and delayed repair on the structure of the muscles of the rotator cuff: an experimental study in sheep. J Bone Joint Surg Am 2004;86:1973-82.
13. Harryman DT 2nd, Mack LA, Wang KY, Jackins SE, Richardson ML, Matsen FA 3rd. Repairs of the rotator cuff. Correlation of functional results with integrity of the cuff. J Bone Joint Surg Am 1991;73:982-9.
14. Hee CK, Dines JS, Dines DM, Roden CM, Wisner-Lynch LA, Turner AS, et al. Augmentation of a rotator cuff suture repair using rhPDGF-BB and a type I bovine collagen matrix in an ovine model. Am J Sports Med 2011;39:1630-9. https://doi.org/10.1177/0363546511404942
15. Kettler A, Liakos L, Haegele B, Wilke HJ. Are the spines of calf, pig and sheep suitable models for pre-clinical implant tests? Eur Spine J 2007;16:2186-92. https://doi.org/10.1007/s00586-007-0485-9
16. Lehman C, Cuomo F, Kummer FJ, Zuckerman JD. The incidence of full thickness rotator cuff tears in a large cadaveric population. Bull Hosp Jt Dis 1995;54:30-1.
17. Lewis CW, Schlegel TF, Hawkins RJ, James SP, Turner AS. Comparison of tunnel suture and suture anchor methods as a function of time in a sheep model. Biomed Sci Instrum 1999;35:403-8.
18. Lewis CW, Schlegel TF, Hawkins RJ, James SP, Turner AS. The effect of immobilization on rotator cuff healing using modified Mason-Allen stitches: a biomechanical study in sheep. Biomed Sci Instrum 2001;37:263-8.
19. Lin JC, Weintraub N, Aragaki DR. Nonsurgical treatment for rotator cuff injury in the elderly. J Am Med Dir Assoc 2008;9:626-32. https://doi.org/10.1016/j.jamda.2008.05.003
20. Loh QL, Choong C. Three-dimensional scaffolds for tissue engineering applications: role of porosity and pore size. Tissue Eng Part B Rev 2013;19:485-502. https://doi.org/10.1089/ten.TEB.2012.0437
21. Lorbach O, Anagnostakos K, Vees J, Kohn D, Pape D. Three-dimensional evaluation of the cyclic loading behavior of different rotator cuff reconstructions. Arthroscopy 2010;26:S95-105. https://doi.org/10.1016/j.arthro.2010.02.006
22. Lorbach O, Bachelier F, Vees J, Kohn D, Pape D. Cyclic loading of rotator cuff reconstructions: single-row repair with modified suture configurations versus double-row repair. Am J Sports Med 2008;36:1504-10. https://doi.org/10.1177/0363546508314424
23. Luan T, Liu X, Easley JT, Ravishankar B, Puttlitz C, Feeley BT. Muscle atrophy and fatty infiltration after an acute rotator cuff repair in a sheep model. Muscles Ligaments Tendons J 2015;5:106-12. https://doi.org/10.11138/mltj/2015.5.2.106
24. McCarron JA, Derwin KA, Bey MJ, Polster JM, Schils JP, Ricchetti ET, et al. Failure with continuity in rotator cuff repair "healing". Am J Sports Med 2013;41:134-41. https://doi.org/10.1177/0363546512459477
25. McGilvray KC, Santoni BG, Turner AS, Bogdansky S, Wheeler DL, Puttlitz CM. Effects of (60)Co gamma radiation dose on initial structural biomechanical properties of ovine bone–patellar tendon–bone allografts. Cell Tissue Bank 2011;12:89-98. https://doi.org/10.1007/s10561-010-9170-z
26. Mellado JM, Calmet J, Olona M, Esteve C, Camins A, Perez Del Palomar L, et al. Surgically repaired massive rotator cuff tears: MRI of tendon integrity, muscle fatty degeneration, and muscle atrophy correlated with intraoperative and clinical findings. AJR Am J Roentgenol 2005;184:1456-63. https://doi.org/10.2214/ajr.184.5.01841456
27. Novakova SS, Mahalingam VD, Florida SE, Mendias CL, Allen A, Arruda EM, et al. Tissue-engineered tendon constructs for rotator cuff repair in sheep. J Orthop Res 2018;36:289-99. https://doi.org/10.1002/jor.23642
28. Pearce AI, Richards RG, Milz S, Schneider E, Pearce SG. Animal models for implant biomaterial research in bone: a review. Eur Cell Mater 2007;13:1-10. https://doi.org/10.22203/ecm.v013a01
29. Peterson DR, Ohashi KL, Aberman HM, Piza PA, Crockett HC, Fernandez JI, et al. Evaluation of a collagen-coated, resorbable fiber scaffold loaded with a peptide basic fibroblast growth factor mimetic in a sheep model of rotator cuff repair. J Shoulder Elbow Surg 2015;24:1764-73. https://doi.org/10.1016/j.jse.2015.06.009
30. Ricchetti ET, Aurora A, Iannotti JP, Derwin KA. Scaffold devices for rotator cuff repair. J Shoulder Elbow Surg 2012;21:251-65. https://doi.org/10.1016/j.jse.2011.10.003
31. Rodeo SA, Potter HG, Kawamura S, Turner AS, Kim HJ, Atkinson BL. Biologic augmentation of rotator cuff tendon-healing

with use of a mixture of osteoinductive growth factors. J Bone Joint Surg Am 2007;89:2485-97. https://doi.org/10.2106/JBJS.C.01627
32. Santoni BG, McGilvray KC, Lyons AS, Bansal M, Turner AS, Macgillivray JD, et al. Biomechanical analysis of an ovine rotator cuff repair via porous patch augmentation in a chronic rupture model. Am J Sports Med 2010;38:679-86. https://doi.org/10.1177/0363546510366866
33. Schlegel TF, Hawkins RJ, Lewis CW, Motta T, Turner AS. The effects of augmentation with Swine small intestine submucosa on tendon healing under tension: histologic and mechanical evaluations in sheep. Am J Sports Med 2006;34:275-80. https://doi.org/10.1177/0363546505279912
34. Schlegel TF, Hawkins RJ, Lewis CW, Turner AS. An in vivo comparison of the modified Mason-Allen suture technique versus an inclined horizontal mattress suture technique with regard to tendon-to-bone healing: a biomechanical and histologic study in sheep. J Shoulder Elbow Surg 2007;16:115-21. https://doi.org/10.1016/j.jse.2006.05.002
35. Seeherman HJ, Archambault JM, Rodeo SA, Turner AS, Zekas L, D'Augusta D, et al. rhBMP-12 accelerates healing of rotator cuff repairs in a sheep model. J Bone Joint Surg Am 2008;90:2206-19. https://doi.org/10.2106/JBJS.G.00742
36. Smith MJ, Pfeiffer FM, Cook CR, Kuroki K, Cook JL. Rotator cuff healing using demineralized cancellous bone matrix sponge interposition compared to standard repair in a preclinical canine model. J Orthop Res 2018;36:906-12. https://doi.org/10.1002/jor.23680
37. Snyder SJ, Burns JP. Rotator cuff healing and the bone marrow "crimson duvet" from clinical observations to science. Tech Shoulder Elbow Surg 2009;10:130-7. https://doi.org/10.1097/bte.0b013e3181c2a940
38. Thangarajah T, Pendegrass CJ, Shahbazi S, Lambert S, Alexander S, Blunn GW. Augmentation of rotator cuff repair with soft tissue scaffolds. Orthop J Sports Med 2015;3. https://doi.org/10.1177/2325967115587495. 2325967115587495.
39. Trappey GJ 4th, Gartsman GM. A systematic review of the clinical outcomes of single row versus double row rotator cuff repairs. J Shoulder Elbow Surg 2011;20:S14-9. https://doi.org/10.1016/j.jse.2010.12.001
40. Turner AS. Experiences with sheep as an animal model for shoulder surgery: strengths and shortcomings. J Shoulder Elbow Surg 2007;16:S158-63. https://doi.org/10.1016/j.jse.2007.03.002
41. Van Kampen C, Arnoczky S, Parks P, Hackett E, Ruehlman D, Turner A, et al. Tissue-engineered augmentation of a rotator cuff tendon using a reconstituted collagen scaffold: a histological evaluation in sheep. Muscles Ligaments Tendons J 2013;3:229-35. https://doi.org/10.1002/jor.23642
42. Vitale MA, Vitale MG, Zivin JG, Braman JP, Bigliani LU, Flatow EL. Rotator cuff repair: an analysis of utility scores and cost-effectiveness. J Shoulder Elbow Surg 2007;16:181-7. https://doi.org/10.1016/j.jse.2006.06.013
43. Wall LB, Keener JD, Brophy RH. Clinical outcomes of double-row versus single-row rotator cuff repairs. Arthroscopy 2009;25:1312-8. https://doi.org/10.1016/j.arthro.2009.08.009
44. Wilke HJ, Kettler A, Claes LE. Are sheep spines a valid biomechanical model for human spines? Spine (Phila Pa 1976) 1997;22:2365-74.
45. Yamaguchi K. New guidelines on rotator cuff problems. Paper presented at: 2011 Annual Meeting of the American Academy of Orthopaedic Surgeons. February 15-19, 2011; San Diego, CA.
46. Yokoya S, Mochizuki Y, Nagata Y, Deie M, Ochi M. Tendon-bone insertion repair and regeneration using polyglycolic acid sheet in the rabbit rotator cuff injury model. Am J Sports Med 2008;36:1298-309. https://doi.org/10.1177/0363546508314416
47. Yoo JC, Ahn JH, Koh KH, Lim KS. Rotator cuff integrity after arthroscopic repair for large tears with less-than-optimal footprint coverage. Arthroscopy 2009;25:1093-100. https://doi.org/10.1016/j.arthro.2009.07.010